Evolution of p53 in hypoxia-stressed *Spalax* mimics human tumor mutation

Osnat Ashur-Fabian*†, Aaron Avivi†‡§, Luba Trakhtenbrot*, Konstantin Adamsky*, Meytal Cohen*, Gadi Kajakaro*, Alma Joel‡, Ninette Amariglio*, Eviatar Nevo‡§, and Gideon Rechavi*

*Pediatric Hematology–Oncology, Safra Children's Hospital, The Chaim Sheba Medical Center, Tel-Hashomer and Sackler School of Medicine, Tel Aviv University, Tel Aviv 69978, Israel; and ‡Institute of Evolution, University of Haifa, Mount Carmel, Haifa 31905, Israel

Contributed by Eviatar Nevo, July 11, 2004

The tumor suppressor gene *p53* controls cellular response to a variety of stress conditions, including DNA damage and hypoxia, leading to growth arrest and/or apoptosis. Inactivation of *p53*, found in 40–50% of human cancers, confers selective advantage under hypoxic microenvironment during tumor progression. The mole rat, *Spalax*, spends its entire life cycle underground at decidedly lower oxygen tensions than any other mammal studied. Because a wide range of respiratory adaptations to hypoxic stress evolved in *Spalax*, we speculated that it might also have developed hypoxia adaptation mechanisms analogous to the genetic/epigenetic alterations acquired during tumor progression. Comparing *Spalax* with human and mouse p53 revealed an arginine (R) to lysine (K) substitution in *Spalax* (Arg-174 in human) in the DNA-binding domain, identical to known tumor associated mutations. Multiple p53 sequence alignments with 41 additional species confirmed that Arg-174 is highly conserved. Reporter assays uncovered that *Spalax* p53 protein is unable to induce apoptosis-regulating target genes, resulting in no expression of *apaf1* and partial expression of *puma*, *pten*, and *noxa*. However, cell cycle arrest and p53 stabilization/homeostasis genes were overactivated by *Spalax* p53. Lys-174 was found critical for *apaf1* expression inactivation. A DNA-free p53 structure model predicts that Arg-174 is important for dimerization, whereas *Spalax* Lys-174 prevents such interactions. Similar neighboring mutations found in human tumors favor growth arrest rather than apoptosis. We hypothesize that, in an analogy with human tumor progression, *Spalax* underwent remarkable adaptive p53 evolution during 40 million years of underground hypoxic life.

The transcription regulation activity of p53, as part of an intracellular nonimmune surveillance mechanism, controls cellular response to a variety of stress conditions, including DNA damage and hypoxia, leading to growth arrest and apoptosis (1, 2). Hypoxia and the resultant metabolic abnormalities induce p53, which in turn, through a specific DNA-binding domain, activates the transcription of multiple genes (3). The cell fate reflects the overall impact of the various genes and pathways regulated by this transcription factor. Some p53-induced genes, such as *p21*, mediate the inhibition of cyclin-dependent kinases and growth arrest, whereas other target genes, such as *bax* and *apaf1*, induce apoptotic cell death. During tumor progression, angiogenesis fails to keep pace, and tumor cells become hypoxic (4, 5). Alteration of *p53*, the most common mutation in human cancers (2, 6), plays an important role in regulating the survival and angiogenic response of tumor cells under hypoxic microenvironments (7).

The Israeli blind subterranean mole rat belongs to the superspecies *Spalax ehrenbergi*. This group of species consists of at least 12 allospecies in the Near East. The four allospecies in Israel were intensively studied interdisciplinarily across all organizational levels (8, 9). They adapted to four different climatic regimes: *Spalax galili* ($2n = 52$) inhabits the cool–humid Upper Galilee Mountains; *Spalax golani* ($2n = 54$), in the cool, semihumid Golan Heights; *Spalax carmeli* ($2n = 58$), in the warm–humid central Israel; and *Spalax judaei* ($2n = 60$), in the warm–dry southern regions. Hypoxia and hypercapnia climax in the northern *S. galili* and *S. golani*, where high rainfall and floods occur during wintertime (8, 9). The entire life cycle of *Spalax* is spent underground in subterranean burrows at decidedly low-oxygen tension. Hypoxia climaxes during winter rains and flooding, when gas solubility and permeability are restricted and the animal is occupied in tunnel rebuilding (8, 9). The critical pO_2 (the lowest oxygen pressure supporting life) is lower for *Spalax* than for any other mammal studied to date (8, 9). We measured 7% O_2 inside the *Spalax* burrows after rains (unpublished data) and in the laboratory, where it can survive at least 14 h under 3% O_2. Under the same conditions, *Rattus* dies after 2–4 h. This capacity to withstand hypoxic conditions exceeds that manifested by many high-altitude and diving mammals. Since its origin some 40 million years ago, *Spalax* has evolved multiple adaptations to underground life that allows it to survive and carry out intense activities in a highly hypoxic environment (8–11), including different structure and function of vascular endothelial growth factor (VEGF) (10), hemoglobin (12), haptoglobin (13), myoglobin (14), erythropoietin, neuroglobin, and cytoglobin (unpublished data).

We speculate that *Spalax* also developed hypoxia adaptation mechanisms that are analogous to the genetic and epigenetic alterations in *p53* acquired by cancer cells during tumor progression. We cloned *Spalax p53* and compared the sequence with that of the germ-line *p53* sequences of humans and mice, as well as to a *p53* tumoral mutation database. Two *Spalax*-specific substitutions in the p53 DNA-binding domain that are identical to known human tumor-associated mutations, altering arginine (R) to lysine (K) in *Spalax*, were discovered at positions corresponding to codons 174 and 209 in human. Further comparison to an additional 41 different species and subspecies indicated that only codon 174 is highly conserved. The impact of these alterations on the transcription activation of several p53 target genes, using reporter assays, indicates a bias toward G_1 arrest versus apoptosis.

Methods

Animals. *Spalax* was captured in the field and housed in individual cages in the animal house of the Institute of Evolution, University of Haifa. Individuals used in this study were *S. galili* ($2n = 52$) from the Kerem Ben Zimra population, *S. golani* ($2n = 54$) from the Quneitra population, *S. carmeli* ($2n = 58$) from the Mt. Carmel population, and *S. judaei* ($2n = 60$) from the Anza population (9). The Ethics Committee of the University of Haifa approved all experiments.

Data deposition: The sequence reported in this paper has been deposited in the GenBank database (accession no. AJ783406).

†O.A.-F. and A.A. contributed equally to this work.

§To whom correspondence may be addressed. E-mail: nevo@research.haifa.ac.il or aaron@esti.haifa.ac.il.

Cloning *Spalax p53*. *Spalax p53* cDNA was cloned from mRNA prepared from a whole embryo belonging to the *S. judaei* species (GenBank accession no. AJ7-83406). Isolation was achieved by using RT-PCR, using oligos at the 5′ and 3′ UTRs, synthesized according to published human (GenBank accession no. NM000546) and mouse (GenBank accession no. NM011640) *p53* sequences.

To confirm the authenticity of the amino acid sequence observed in the binding domain of *Spalax* p53, this region was further cloned from spleen mRNA of one adult from each of the four different Israeli *Spalax* species, using RT-PCR and *Spalax*-specific oligos flanking the *Spalax p53*-binding domain.

Plasmids. For transfection studies, we constructed expression plasmids of the human *p53*, human mutated *p53*, and *Spalax p53*. Human wild-type *p53* was ligated into a pCMV (cytomegalovirus) construct. Two different human mutated *p53* constructs (H179R and 342-stop) were generated by using QuikChange XL site-directed mutagenesis kit following the manufacturer's instructions (Stratagene). *Spalax p53* was ligated into a pCDNA3 expression vector. Different luciferase constructs containing the p53 response elements of *apaf1* (15), *bax*, *puma*, *noxa*, *cycG*, *p21*, *pten*, and *mdm2* (a generous gift of M. Oren, Weizmann Institute of Science, Rehovot, Israel) were used.

Cell Cultures. U2OS (human osteosarcoma, ATCC CRL-5803) and H1299 (human non-small cell lung cancer, ATCC HTB-96) were grown in 10% FCS in DMEM (GIBCO/BRL) or RPMI medium 1640 (Sigma), respectively, supplemented with 2 mM glutamine, 100 μg/ml streptomycin, and 100 units/ml penicillin (GIBCO/BRL) at 37°C in a humidified incubator with 5% CO_2.

Transient Transfection. Transient transfection assays were performed on H1299 and U2OS cell lines, using JetPEI transfection reagent (Polyplus Transfection, Ilkirch, France). Cells were plated at 250,000 cells per well in 12-well plates. One day (24 h) after plating, the medium was replaced by 0.5 ml of serum-free medium and a mixture of the various luciferase reporter constructs containing the human promoters of several p53 target genes (500 ng, pGL2-basic vector, Promega), and *p53* plasmids (1 μg, pCDNA3 and pCMV vector) were added for 5 h, after which the medium was changed back to one containing 10% FCS. Dual luciferase reporter assay system (Promega) was used with results normalized to *Renilla* luciferase assay system (cytomegalovirus vector, Promega). The next day, plates were washed twice with cold PBS, collected, and immediately taken for quantification in a luminometer.

Humanization of the *Spalax p53* Plasmids. The exchange of arginine instead of lysine at positions 172 and 207 (positions 174 and 209 in humans) of the wild-type *Spalax p53* plasmid was done by using the QuikChange XL site-directed mutagenesis kit following manufacturer instructions (Stratagene). The amino acid changes were introduced into the plasmid by using the following primers: K172R forward, 5′-GAC AGA AGT TGT AAG GCG CTG CCC CCA CC-3′; K172R reverse, 5′-GGT GGG GGC AGC GCC TTA CAA CTT CTG TC-3′; K207R forward, 5′-GCA GAG TAT TTG GAT GAC AGG CAC ACT TTT CGA CAC-3′; K207R reverse, 5′-GTG TCG AAA AGT GTG CCT GTC ATC CAA ATA CTC TGC-3′ (underlines indicate the exchanges made for "humanization" of *Spalax p53*).

Three-Dimensional Structure Analysis of *Spalax p53*. The structure of the DNA-binding domain of *Spalax* p53 was modeled with the homology-modeling program NEST (16), using the template structure of DNA-bound human p53 (16) (Protein Data Bank ID code 1TSR). The NEST program was also used for modeling a dimer of the DNA-binding domain of *Spalax* based on the dimer that comprises the free-DNA monomer and bound-DNA monomer seen in the crystal structure of human p53 (17). A second dimer was modeled based on a dimer seen in the mouse p53 crystal structure (18) (Protein Data Bank ID Code 1HU8). The solvent-accessible surface areas were calculated by using the SURFV program.[¶] Superimpositions of structures were made by using the C-ALPHA MATCH program (20, 21) and INSIGHTII (Accelrys, San Diego). Pictures were made by using MOLSCRIPT (22) and RASTER 3D (23).

Phylogenetic Tree. A phylogenetic tree was computed by using the neighbor-joining method (24) based on Jukes–Cantor distances.

Multiple Alignment Tools. For comparing the p53 protein of 44 different species a multiple sequence alignment was generated by using MULTALIN (http://prodes.toulouse.inra.fr/multalin/multalin.html; ref. 25). For the phylogenetic tree, a multiple sequence alignment (MSA) of the DNA-binding domain of 36 p53's orthologues was constructed by using CLUSTALW (26).

***p53* Mutation database.** For p53 mutation database, International Agency for Research on Cancer TP53 database (www.iarc.fr/p53/index.html; version R8, June 2003) was used (27).

Results

Comparing the *p53* Sequences of *Spalax*, Mouse, and Human. *Spalax p53* was cloned, sequenced, and compared with the known human and mouse *p53* mRNAs and proteins. *Spalax p53* mRNA is 1,368 bases long, translated into a 391-aa protein, with 83.7% homology to human and 82.2% to mouse *p53* mRNA. At the amino acid level, an identity of 85.4% to human and 81.9% to mouse p53 proteins is observed. In the *p53* DNA-binding domain region (Fig. 1), there is a nucleotide sequence homology of 88.1% to humans and 86.1% to mice, whereas amino acid homology is 95.8% for humans and 89.5% for mice.

Multiple alignment analysis (http://prodes.toulouse.inra.fr/multalin/multalin.html; ref. 25) revealed that, in the DNA-binding region, two amino acids differentiate *Spalax* from human and mouse sequences (Fig. 1). The bases at positions 515 and 620 from the transcription-starting site of *Spalax* mRNA sequence are adenosine (A) bases, whereas a guanine (G) is present in the human and mouse. Thus, lysine (Lys, AAG) is coded at positions 172 and 207 in *Spalax* p53 protein (corresponds to codons 174 and 209 in human p53), and arginine (Arg, AGG/AGA) is coded in the human and mouse p53 proteins.

p53 Target Genes Activation: Human Versus *Spalax*. One of the major functions of p53 is its ability to bind to and activate several target genes. Because mutant forms of p53 may have different effects, we investigated the ability of *Spalax* wild-type p53 to activate the transcription of several human target genes. For this analysis, expression plasmids carrying either *Spalax* or human wild-type *p53* coding regions were used. Two mutated human *p53* plasmids were used as controls: mut179 (H179R) and Mut342-stop (342R). *Spalax* homologues of p53 target genes have not been cloned; therefore, several human promoter constructs were used. Transient transfections were performed on U2OS (without induction of endogenous wild-type *p53*) and H1299 (*p53*-null) human cell lines. Luciferase assays for eight different human p53 target genes, including *apaf1*, *mdm2*, *bax*, *puma*, *noxa*, *cycG*, *p21*, and *pten*, were performed. The targets selected are known to be involved in different pathways, including cell cycle arrest, apoptosis, and stabilization/homeostasis of the p53 protein. The relative transactivation capacities of the different *p53* plasmids toward the eight target genes (Fig. 2) are summarized with

[¶]Sridharan, S., Nicholls, A. & Honig, B. (1992) *Biophys. J.* **61,** A174 (abstr.).

EVOLUTION

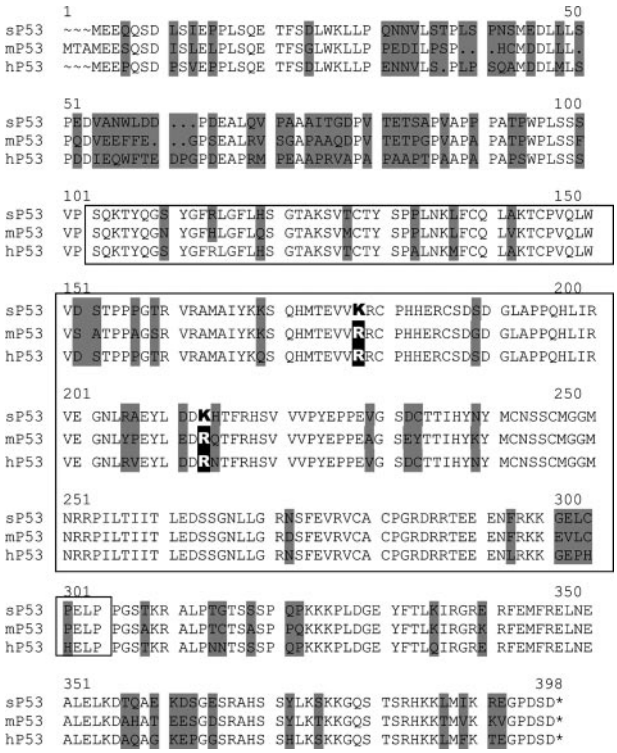

Fig. 1. Sequence of *Spalax* p53. Amino acid sequence alignment of *Spalax* (sp53), mouse (mp53), and human (hp53), with full-length p53 proteins (http://prodes.toulouse.inra.fr/multalin/multalin.html; ref. 25). The DNA-binding domain is shown in a box. Identities of species are in a white background. Changes among the species are in a gray background. *Spalax*-specific changes are depicted in bold black letters, and the amino acids common to other species are in bold white letters in a black background.

respect to wild-type human *p53* (detailed luciferase assays are shown in Fig. 5, which is published as supporting information on the PNAS web site).

Overall, four different activation patterns were observed. *Apaf1* promoter, although activated by the human wild-type p53,

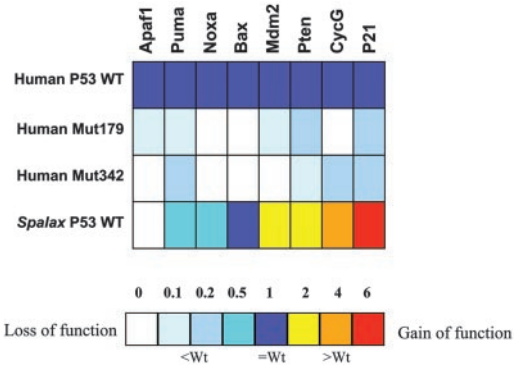

Fig. 2. Relative transactivation of eight different human promoters. Human wild-type p53, mutated p53 (mut179 and mut342), and *Spalax* p53 were examined relative to an array of p53 target gene promoters. The relative transactivation with respect to human wild-type p53 is presented in a form similar to that of expression microarrays, ranging from complete loss of function (white) to a 6-fold increase of activation (red). Human wild-type p53 presents 1-fold of activation (blue), and other levels of transactivation are presented as shaded colors ranging from white (loss of function) to red (gain of function). Results are mean ± SE of four to eight independent transient transfections performed in triplicate (*P* value, unpaired *t* test).

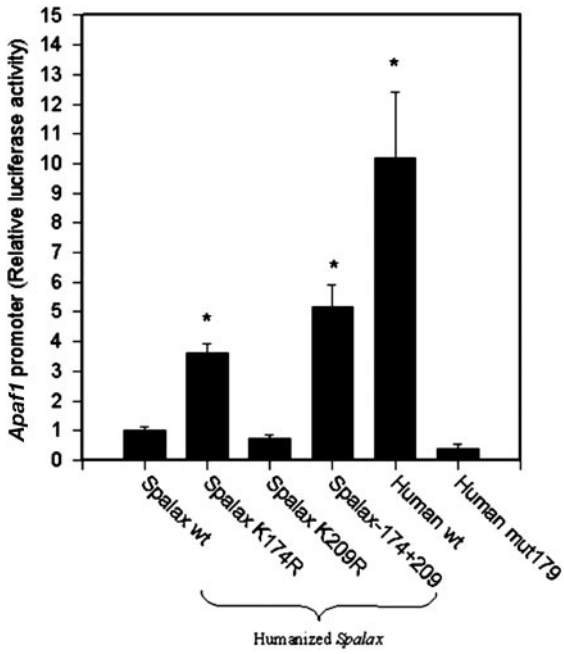

Fig. 3. *Spalax* wild-type and humanized *p53* ability to transactivate *Apaf1* promoter, with respect to human wild-type and mutated p53. Results are normalized to *Renilla*-luciferase and presented as fold-change from *Spalax* wild type (depicted as 1-fold of activation). Results are mean ± SE of four independent transfection assays, performed in triplicate *, $P < 0.005$ (unpaired *t* test).

was not responsive to *Spalax* wild-type p53. *Spalax* p53 ability to activate the promoters of the proapoptotic genes *noxa* and *puma* was lower than that of the human p53 (≤0.5-fold of activation compared with human wild-type, $P < 0.015$) and similar to human wild-type p53 in regard to *bax* (0.98-fold of activation, $P = 0.051$). Increased activation of the promoters of *pten* and *mdm2* by *Spalax* p53 protein was observed (up to 2-fold of activation compared with the human wild-type p53, $P < 0.05$), with an even greater impact on *cycG* and *p21* promoters (4- and 6-fold of activation, respectively, $P < 0.0015$). The mutated human p53 used as negative controls resulted in a partial or complete loss of function in regard to all targets tested.

Humanizing *Spalax* p53 by Site-Directed Mutagenesis. To test whether the lysines in *Spalax* p53 protein are responsible for the inability to activate *apaf1* promoter, *Spalax* p53 protein was humanized by using site-directed mutagenesis, changing amino acid lysine (K) to arginine (R) at positions 172 and/or 207 (corresponding to positions 174 and 209 in humans). Cotransfections with human *apaf1* promoter luciferase construct, together with the different *p53 Spalax* plasmids (wild-type and humanized) were performed. Human wild-type and mutated *p53* were used as controls. Humanization of *Spalax p53* at position 174 resulted in a 3-fold increased activation of the *apaf1* promoter (Fig. 3), whereas substituting lysine to arginine at position 209 did not have any effect, giving similar results as the original *Spalax* wild-type p53 protein. A synergistic effect was observed when both amino acids were altered to the human sequence, giving a 5-fold increased activation compared with the original *Spalax* wild-type p53 protein and 50% of the activity exhibited by human wild-type p53.

Crystallography-Based Models of *Spalax*, Human, and Mouse p53. The structure of *Spalax* p53 was predicted, based on the human and mouse p53 models, to understand the role of *Spalax*-specific

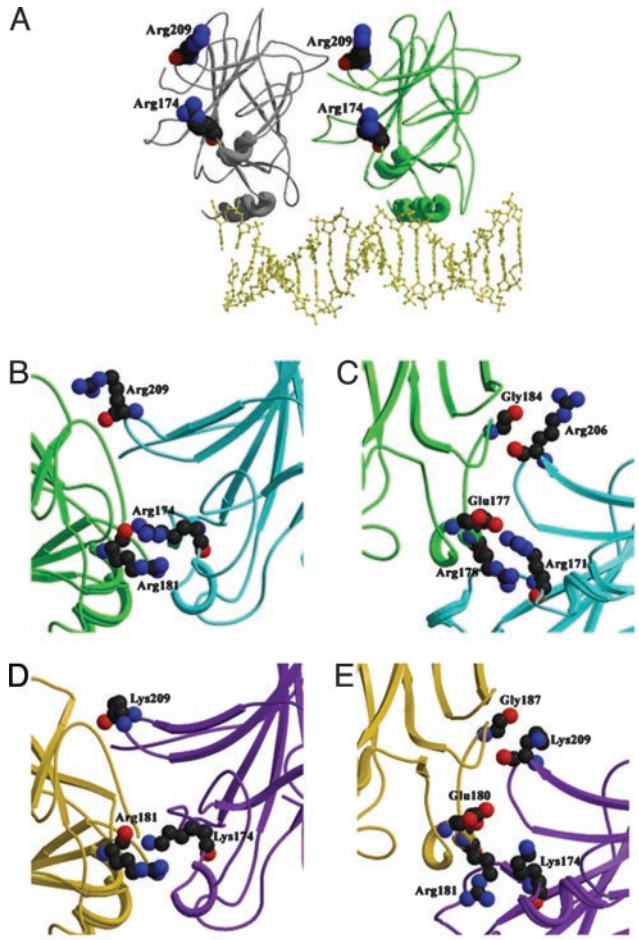

Fig. 4. Three-dimensional models of human, mouse, and *Spalax* proteins. (*A*) DNA-bound human p53 model. Arg-174 and Arg-209 are not located in or near the DNA-binding site and, thus, have no effect on the protein fold and/or stabilization in the DNA bound state. (*B–E*) Protein–protein interaction between p53 DNA-binding domain monomers. Residues 174 (171 in the mouse) and 209 (206 in the mouse) and residues contacting them on the adjacent monomers are represented as ball-and-stick structures, colored by atom type (carbon in black, oxygen in red, and nitrogen in blue). (*B*) The human *p53* dimer is displayed as cyan and green ribbons. Arg-174 contacts Arg-181 on the adjacent monomer. (*C*) The mouse P53 dimer (*Left*) is displayed as light blue and green ribbons. Arg-171 contacts Arg-178 on the adjacent monomer and is in close proximity to Glu-177. The modeled *Spalax* p53 dimer (purple and gold ribbons, *Right*) is shown in the same orientation as the human (*D*) and mouse (*E*) P53 dimer. The smaller Lys-174 displays different interaction within the interface, leading to a changed dimer configuration; thus, the dimer shown in the figure could not be preserved. Lys-209 is not involved in contacting the adjacent monomer displaying fewer contacts with Gly-181/Gly-187 on the adjacent monomers in humans and mice, respectively, with only a minor affect on the interface.

arginine-to-lysine amino acid changes at codons 174 (171 in mouse) and 209 (206 in mouse). According to human and mouse p53 crystallography-based models, it is established that p53 generates two types of dimers: one that binds DNA through the DNA-binding domain and a second type that is formed before the DNA contact (17, 18, 28).

In the DNA-bound human p53 model (Fig. 4*A*), Arg-174 and Arg-209 are not located near the DNA-binding site and thus are not involved in stabilizing the folding of the protein. However, according to the DNA-free human and mouse models (Fig. 4 *B* and *C*, respectively), Arg-174 contacts residues in the adjacent monomer, mainly Arg-181 (178 in mouse). This contact between two positively charged residues is stabilized by hydrophobic interactions within the arginine side chains and a nearby negatively charged Glu-180 in humans (177 in mice). In the p53 monomer, Arg-174 and -209 are exposed to the surface. By contrast, in the dimer conformation, the surface area of Arg-174 is buried in the dimer, 58% in humans and 85% in mice, whereas Arg-209 only partially participated in the interface, with 13% buried in the dimer in the mouse and totally exposed in the human. Interestingly, in *Spalax*, the smaller Lys-174 is incapable of mediating the same interactions as the human/mouse Arg-174/171 (Fig. 4 *D* and *E*, respectively); thus, the *Spalax*-formed dimer is unstable and probably adapts to a different contact area.

Discussion

p53 Mutations in Human Cancer and in Underground-Adapted *Spalax*. Cells exposed to hypoxic conditions accumulate wild-type p53 protein and succumb to apoptotic cell death (29). In human cancer, wild-type p53 expression is often abrogated by somatic mutations. In fact, >50% of human tumors carry mutations in the *p53* gene (1, 30). Hypoxia was suggested as a selection pressure for mutating *p53* of solid tumors during conversion into ascite tumors, making the cells less prone to hypoxia-induced apoptosis (29, 31). *Spalax* is a blind mole rat that spends its life underground. Primarily during winter floods, it is exposed to extreme hypoxic conditions (8, 9). We hypothesized that this genus adapts to the extreme hypoxic condition by a battery of adaptive genes (8, 9) involving mutations in the *p53* gene, analogous to *p53* mutations acquired during tumor progression. This hypothesis is supported by our previous results (10) indicating that *Spalax* vascular endothelial growth factor (*VEGF*) expression is similar to its expression in cancer growths. Similar to *VEGF* expression pattern in human tumors, *Spalax VEGF* is constitutively expressed in maximal levels under normoxia, with no further increase under hypoxia. Here, we cloned the *Spalax p53* mRNA and used reporter assays to establish that *Spalax* p53 protein is functionally biased toward G_1 arrest activation and impaired toward apoptosis target genes.

The *Spalax* p53 Lysine Adaptation Mimics Tumor Evolution. The *Spalax*-specific modifications observed within the p53 DNA-binding domain replace arginine (R) with lysine (K) in the *Spalax* p53 protein (corresponding to codons 174 and 209 in humans). Arginine at codon 174 is reported to be affected in 57 different tumors of various types (www.iarc.fr/p53/index.html), with an identical arginine-to-lysine exchange in eight different human cancers, including medulloblastoma (32), squamous cell carcinomas of the head and neck (33), oral cancer (34), breast cancer (35), colon cancer (36), ovary adenocarcinoma (37), lung cancer (38, 39), and liver cancer (40). Moreover, this specific mutation was reported in canine thyroid carcinoma (41). Arginine at codon 209 is mutated in 69 tumors, among which five of these tumors harbor the exact arginine-to-lysine alteration including B cell chronic lymphocytic leukemia (42), esophageal carcinoma (43), skin cancer (44), uterine cervical cancer (45), and colon cancer (46).

***Spalax* p53 Favors Growth Arrest, but Not Apoptotic Target Genes.** A large-scale p53 mutation analysis research published recently (47) concluded that three p53 mutant subtypes exist: mutants with no activity (9.6%), mutants with significantly reduced activity but some residual activity (26.5%), and mutants that retain wild-type activity (63.9%). According to these categories, *Spalax* p53 protein is a partially inactivated protein version, working in a similar manner to several known p53 mutations, favoring the promoters of cell cycle arrest genes rather than apoptotic targets. *Apaf1* promoter, a central-player in the mitochondrial apoptotic pathway, recently described by our group and others (15, 48, 49) as a p53 primary target, was completely inactivated by *Spalax* p53. Interestingly, a neighboring mutated

V173L was also incapable of activating *Apaf1* promoter (49). Remarkably, however, the same *Spalax* p53 protein overactivated targets involved in cell cycle and p53 stabilization/homeostasis, including *p21*, *cycG*, *pten*, and *mdm2* (Figs. 2 and 5). Such results were obtained with 143A, 175P, and 181L human p53 mutants, retaining the ability to transactivate *p21* reporter but failing to activate apoptotic target genes, including *bax* (143A and 175P) and *IGF-BP3* (143A, 175P and 181L) (50). Furthermore, it was previously reported that several mutations of arginine at codon 175 to leucine (28), isoleucine, or serine (51) ablate apoptosis activity but function as a wild type in regard to cell cycle arrest. This phenomenon was also observed at codon 175 mutated from arginine to lysine, the same amino acid alteration observed within *Spalax* p53 protein (51). Recently, a mouse model was described (52) in which a p53 R175P mutation was introduced. This mutation, neighboring codon 174, which was studied by us, was also defective in initiating apoptosis while still inducing cell cycle arrest.

Several lines of evidence demonstrate that cell cycle arrest and apoptosis are separate p53 functions, with accumulating reports regarding *p53* mutants that are able to induce cell cycle arrest while failing to activate apoptosis. The common concept that might explain observations of such differential activities is that cell cycle arrest targets of p53, such as *p21*, seem to be more efficiently activated than apoptotic targets (53).

Highlighting Spalax p53 Adaptation by 3D Models. The residues in the p53 DNA-binding domain that either directly contact DNA or closely contact those that do so are the most often mutated (54). As such, arginine at codon 175, neighboring the Arg-174 altered in *Spalax*, located in the L2 loop near the zinc-binding site of the p53 protein (54–56), is one of the hot spots for mutation in human cancers.

Three-dimensional analyses based on human and mouse p53 protein models were conducted to understand the effect of *Spalax*-specific amino acid changes. Previous human and mouse p53 crystallography-based models established that p53 generates two types of dimers: one that binds DNA through the DNA-binding domain and a second one, which is a non-DNA-bound dimer, that forms before the DNA contact (17, 18, 28, 57). When p53 is bound to DNA, a *Spalax* lysine-to-arginine alteration at codons 174 and 209 is not located in or near the DNA-binding site and thus has no effect on the protein fold and stabilization. These characteristics allow the replacement of arginine by lysine in *Spalax* p53 protein without totally abolishing its function, as confirmed by functionality assays conducted in this work (Fig. 2). The H179R p53 mutation, used as a control in our reporter assays, located in a critical zinc-binding region (17), results in a complete loss of function in regard to all promoters tested (Fig. 2). However, in the non-DNA-bound transition state, although Arg-209 plays a minor role, Arg-174 is essential to protein–protein interactions. We suggest that the Lys-174 in *Spalax* p53 protein assumes, before DNA binding, a dimer conformation that results in the activation of different p53 target genes when compared with human p53. Moreover, the ability of the same protein to differentially express a variety of responsive elements, as demonstrated in our work and by others, may be explained by divergent affinities of the same non-DNA-bound state of the p53 dimer toward the various target gene DNA strands.

Comparative p53 DNA-Binding Domain Across Animal Species. According to all data presented in our work concerning activation of the *Apaf1* promoter, the importance of the arginine-to-lysine alteration at codon 174 in comparison with codon 209 was established. These results were further confirmed when a large-scale multiple alignment analysis was conducted between *Spalax* and a spectrum of 41 other species besides humans and mice (Fig. 6 and Table 1, which are published as supporting information on the PNAS web site). According to the multiple alignments conducted, the p53 DNA-binding domain is highly conserved among the different species and subspecies examined. In evolution, sequences coding for the most critical structural or functional amino acids are the most highly conserved because of selection pressures against functionality-altered proteins. Previous comparisons between species indicated five highly conserved regions in the p53 protein (58). The arginine at codon 174 is situated in the third conserved region, characterized as a hotspot for missense mutations (59). Furthermore, multiple alignment performed among 44 species indicated that the amino acid at position 209 in human, originally assumed to be *Spalax*-specific when comparing *Spalax* with humans and mice (Fig. 1), is not a *Spalax*-unique change. Actually, there is a vast variability at this nonconserved region, with 10 different amino acid possibilities among the species examined (Fig. 7, which is published as supporting information on the PNAS web site).

Focusing on the region surrounding the amino acid at codon 174 (Fig. 7) revealed that this amino acid is conserved as arginine (R) among 38 of the species, whereas only *Spalax* and six other species carry a lysine (K) residue at this position. These species include *Xenopus* (African frog), *Monodelphis domestica* (opossum), two species of *Xiphophorus* (tropical fish), *Loligo forbesi* (squid), and *Mya arenaria* (softshell clam). All of these species, except the opossum, live in hypoxic aquatic and/or muddy bottoms.

Intriguingly, in the group containing the R174K alteration, four species are commonly used as animal models for melanoma, including *M. domestica* (South American opossum), *M. arenaria* (60), and a hybrid of two *Xiphophorus* species, the *helleri* and *maculatus* (61). *M. domestica* and the *Xiphophorus* rarely develop melanoma in the wild, but melanoma can be induced by UV irradiation. These species are among the very few animals in which melanoma can be induced by UV alone. The *Xiphophorus* is also actively used as a genetic model organism for the study of neuroblastoma, retinoblastoma, and other malignancies; however, this system is ultimately limited by its evolutionary distance from mammals (62).

Concerning *Xenopus laevis* and *Loligo forbesi*, two aquatic species, the *Xenopus* is submerged for long periods of time, thus making standard inhalation techniques impractical (63), and *Loligo forbesi* lives in deep water (250–500 m) (64). According to a phylogenetic tree conducted on the p53 DNA-binding domain of *Spalax* and 35 other species (Fig. 8, which is published as supporting information on the PNAS web site), *Spalax* is genetically closer to humans and primates than other species examined. Note that similar results were found for other *Spalax* proteins, including CLOCK (65), Per3 (66), CRY1 (67), and HLA (8), indicating the old origin of *Spalax* among rodents (8, 9), closer to the primate junction.

Conclusions

To conclude, p53 controls the expression of multiple target genes, and it is therefore considered to be a master gene of diversity, providing the economic creation of multiple germ-line phenotypes (57). Clearly, as observed by various p53 tumor mutant forms along with *Spalax* p53 reported by us, a single amino acid change could have diverse effects on the ability of p53 to induce the transcription of different target genes. Examples of specific tumoral p53 mutations acquired in response to various environmental stresses are well documented, including exposure to sunlight with skin cancer and tobacco smoking with lung cancer (19). It might be assumed that various p53 mutations may be related to specific types of cancer, such as in UV-induced skin cancer of mice in which a T122L mutation is frequently noticed (57). As such, it is a challenge to establish a connection between the stressful hypoxic underground environments of *Spalax* and the specific amino acid alteration observed in this genus.

Since its origin some 40 million years ago, *Spalax* has evolved adaptations to underground life that allow it to survive and carry out intense activities in a highly hypoxic environment (8, 9). We believe that such adaptive mechanisms for hypoxia, analogous to the genetic and epigenetic alterations acquired by cancer cells during tumor development, are demonstrated in *Spalax* p53 in the present study. We suggest that *Spalax* holds a promising model for the study of malignancies, highlighting the importance of a large-scale *Spalax*-genome project in the near future. This may lead to a better understanding of hypoxia stress tolerance and to the elucidation of malignancy evolution and suppression.

This study is in honor of the late Professor N. N. Vorontsov, a great scientist and distinguished evolutionist. We thank G. Klein, H. Werner, E. Feinstein, and N. Minsky for comments improving the paper. We thank the Arison family for their donation to the Center of DNA Chips in Pediatric Oncology, Chaim Sheba Medical Center. G.R. holds the Djerassi Chair in Oncology at the Sackler School of Medicine. This work was supported by the Ancell Teicher Research Foundation for Genetics and Molecular Evolution.

1. Klein, G. (2004) *Cell Death Differ.* **11,** 13–17.
2. Vousden, K. H. & Lu, X. (2002) *Nat. Rev. Cancer* **2,** 594–604.
3. Levine, A. J. (1997) *Cell* **88,** 323–331.
4. Graeber, T. G., Osmanian, C., Jacks, T., Housman, D. E., Koch, C. J., Lowe, S. W. & Giaccia, A. J. (1996) *Nature* **379,** 88–91.
5. Kinzler, K. W. & Vogelstein, B. (1996) *Nature* **379,** 19–20.
6. Hollstein, M., Sidransky, D., Vogelstein, B. & Harris, C. C. (1991) *Science* **253,** 49–43.
7. Royds, J. A., Dower, S. K., Qwarnstrom, E. E. & Lewis, C. E. (1998) *Mol. Pathol.* **51,** 55–61.
8. Nevo, E. (1999) *Mosaic Evolution of Subterranean Mammals: Regression, Progression and Global Convergence* (Oxford Univ. Press, Oxford).
9. Nevo, E., Ivanitskaya, E. & Beiles, A. (2001) *Adaptive Radiation of the Blind Subterranean Mole Rats* (Backhuys, Leiden, The Netherlands)
10. Avivi, A., Resnick, M. B., Nevo, E., Joel, A. & Levy, A. P. (1999) *FEBS Lett.* **452,** 133–140.
11. Widmer, H. R., Hoppeler, H., Nevo, E., Taylor, C. R. & Weibel, E. R. (1997) *Proc. Natl. Acad. Sci. USA* **94,** 2062–2067.
12. Kleinschmidt, T., Nevo, E. & Braunitzer, G. (1984) *Hoppe-Seylers Z. Physiol. Chem.* **365,** 531–536.
13. Nevo, E., Ben-Shlomo, R. & Maeda, N. (1989) *Heredity* **62,** 85–90.
14. Gurnett, A. M., O'Connell, J., Harris, D. E., Lehmann, H., Joysey, K. A. & Nevo, E. (1984) *J. Prot. Chem.* **3,** 445–454.
15. Rozenfeld-Granot, G., Krishnamurthy, J., Kannan, K., Toren, A., Amariglio, N., Givol, D. & Rechavi, G. (2002) *Oncogene* **21,** 1469–1476.
16. Petrey, D., Xiang, Z., Tang, C. L., Xie, L., Gimpelev, M., Mitros, T., Soto, C. S., Goldsmith-Fischman, S., Kernytsky, A., Schlessinger, A., *et al.* (2003) *Proteins* **53,** 430–435.
17. Cho, Y., Gorina, S., Jeffrey, P. D. & Pavletich, N. P. (1994) *Science* **265,** 346–355.
18. Zhao, K., Chai, X., Johnston, K., Clements, A. & Marmorstein, R. (2001) *J. Biol. Chem.* **276,** 12120–12127.
19. Bennett, W. P., Hussain, S. P., Vahakangas, K. H., Khan, M. A., Shields, P. G. & Harris, C. C. (1999) *J. Pathol.* **187,** 8–18.
20. Bachar, O., Fischer, D., Nussinov, R. & Wolfson, H. A. (1993) *Protein Eng.* **6,** 279–288.
21. Fischer, D., Bachar, O., Nussinov, R. & Wolfson, H. (1992) *J. Biomol. Struct. Dyn.* **9,** 769–789.
22. Kraulis, P. J. (1991) *J. Appl. Crystallogr.* **24,** 946–950.
23. Merritt, E. A. & Bacon, D. J. (1997) *Methods Enzymol.* **277,** 505–524.
24. Saitou, N. & Nei, M. (1987) *Mol. Biol. Evol.* **4,** 406–425.
25. Corpet, F. (1988) *Nucleic Acids Res.* **16,** 10881–10890.
26. Thompson, J. D., Higgins, D. G. & Gibson, T. J. (1994) *Nucleic Acids Res.* **22,** 4673–4680.
27. Olivier, M., Eeles, R., Hollstein, M., Khan, M. A., Harris, C. C. & Hainaut, P. (2002) *Hum. Mutat.* **19,** 607–614.
28. Klein, C., Planker, E., Diercks, T., Kessler, H., Kunkele, K. P., Lang, K., Hansen, S. & Schwaiger, M. (2001) *J. Biol. Chem.* **276,** 49020–49027.
29. Magnusson, K. P., Satalino, R., Qian, W., Klein, G. & Wiman, K. G. (1998) *Oncogene* **17,** 2333–2337.
30. Hernandez, I., Maddison, L. A., Wei, Y., DeMayo, F., Petras, T., Li, B., Gingrich, J. R., Rosen, J. M. & Greenberg, N. M. (2003) *Mol. Cancer Res.* **1,** 1036–1047.
31. Achison, M. & Hupp, T. R. (2003) *Oncogene* **22,** 3431–3440.
32. Wang, W., Kumar, P., Wang, W., Whalley, J., Schwarz, M., Malone, G., Haworth, A. & Kumar, S. (1998) *Anticancer Res.* **18,** 849–853.
33. Caamano, J., Zhang, S. Y., Rosvold, E. A., Bauer, B. & Klein-Szanto, A. J. (1993) *Am. J. Pathol.* **142,** 1131–1139.
34. Kim, M. S., Li, S. L., Bertolami, C. N., Cherrick, H. M. & Park, N. H. (1993) *Anticancer Res.* **13,** 1405–1413.
35. Glebov, O. K., McKenzie, K. E., White, C. A. & Sukumar, S. (1994) *Cancer Res.* **54,** 3703–3709.
36. Heide, I., Thiede, C., Sonntag, T., de Kant, E., Neubauer, A., Jonas, S., Peter, F. J., Neuhaus, P., Herrmann, R., Huhn, D., *et al.* (1997) *Eur. J. Cancer* **33,** 1314–1322.
37. Tavassoli, M., Steingrimsdottir, H., Pierce, E., Jiang, X., Alagoz, M., Farzaneh, F. & Campbell, I. G. (1996) *Br. J. Cancer* **74,** 115–119.
38. Vega, F. J., Iniesta, P., Caldes, T., Sanchez, A., Lopez, J. A., de Juan, C., Diaz-Rubio, E., Torres, A., Balibrea, J. L. & Benito, M. (1997) *Br. J. Cancer* **76,** 44–51.
39. Sanchez-Pernaute, A., Torres, A., Iniesta, P., Hernando, F., Gomez, A., Gonzalez, O., De Juan, C., Perez-Aguirre, E., Maestro, M. L., Lopez-Asenjo, J. A., *et al.* (1998) *Oncol. Rep.* **5,** 1129–1133.
40. Iwamoto, K. S., Fujii, S., Kurata, A., Suzuki, M., Hayashi, T., Ohtsuki, Y., Okada, Y., Narita, M., Takahashi, M., Hosobe, S., *et al.* (1999) *Carcinogenesis* **20,** 1283–1291.
41. Devilee, P., Van Leeuwen, I. S., Voesten, A., Rutteman, G. R., Vos, J. H. & Cornelisse, C. J. (1994) *Anticancer Res.* **14,** 2039–2046.
42. el Rouby, S., Thomas, A., Costin, D., Rosenberg, C. R., Potmesil, M., Silber, R. & Newcomb, E. W. (1993) *Blood* **82,** 3452–3459.
43. Ribeiro, U., Jr., Finkelstein, S. D., Safatle-Ribeiro, A. V., Landreneau, R. J., Clarke, M. R., Bakker, A., Swalsky, P. A., Gooding, W. E. & Posner, M. C. (1998) *Cancer* **83,** 7–18.
44. Zerp, S. F., van Elsas, A., Peltenburg, L. T. & Schrier, P. I. (1999) *Br. J. Cancer* **79,** 921–926.
45. Wistuba, I. I., Thomas, B., Behrens, C., Onuki, N., Lindberg, G., Albores-Saavedra, J. & Gazdar, A. F. (1999) *Gynecol. Oncol.* **72,** 3–9.
46. Iinuma, H., Okinaga, K., Adachi, M., Suda, K., Sekine, T., Sakagawa, K., Baba, Y., Tamura, J., Kumagai, H. & Ida, A. (2000) *Int. J. Cancer* **89,** 337–344.
47. Kato, S., Han, S. Y., Liu, W., Otsuka, K., Shibata, H., Kanamaru, R. & Ishioka, C. (2003) *Proc. Natl. Acad. Sci. USA* **100,** 8424–8429.
48. Kannan, K., Kaminski, N., Rechavi, G., Jakob-Hirsch, J., Amariglio, N. & Givol, D. (2001) *Oncogene* **20,** 3449–3455.
49. Moroni, M. C., Hickman, E. S., Denchi, E. L., Caprara, G., Colli, E., Cecconi, F., Muller, H. & Helin, K. (2001) *Nat. Cell Biol.* **3,** 552–558.
50. Gagnebin, J., Kovar, H., Kajava, A. V., Estreicher, A., Jug, G., Monnier, P. & Iggo, R. (1998) *Oncogene* **16,** 685–690.
51. Ryan, K. M. & Vousden, K. H. (1998) *Mol. Cell. Biol.* **18,** 3692–3698.
52. Liu, G., Parant, J. M., Lang, G., Chau, P., Chavez-Reyes, A., El-Naggar, A. K., Multani, A., Chang, S. & Lozano, G. (2004) *Nat. Genet.* **36,** 63–68.
53. Inga, A., Storici, F., Darden, T. A. & Resnick, M. A. (2002) *Mol. Cell. Biol.* **22,** 8612–8625.
54. Walker, D. R., Bond, J. P., Tarone, R. E., Harris, C. C., Makalowski, W., Boguski, M. S. & Greenblatt, M. S. (1999) *Oncogene* **18,** 211–218.
55. Nikolova, P. V., Henckel, J., Lane, D. P. & Fersht, A. R. (1998) *Proc. Natl. Acad. Sci. USA* **95,** 14675–14680.
56. Tada, M., Iggo, R. D., Waridel, F., Nozaki, M., Matsumoto, R., Sawamura, Y., Shinohe, Y., Ikeda, J. & Abe, H. (1997) *Mol. Carcinog.* **18,** 171–176.
57. Resnick, M. A. & Inga, A. (2003) *Proc. Natl. Acad. Sci. USA* **100,** 9934–9939.
58. Soussi, T., Caron de Fromentel, C. & May, P. (1990) *Oncogene* **5,** 945–952.
59. Greenblatt, M. S., Bennett, W. P., Hollstein, M. & Harris, C. C. (1994) *Cancer Res.* **54,** 4855–4878.
60. Kelley, M. L., Winge, P., Heaney, J. D., Stephens, R. E., Farell, J. H., Van Beneden, R. J., Reinisch, C. L., Lesser, M. P. & Walker, C. W. (2001) *Oncogene* **20,** 748–758.
61. Kazianis, S., Gan, L., Della Coletta, L., Santi, B., Morizot, D. C. & Nairn, R. S. (1998) *Gene* **212,** 31–38.
62. Jhappan, C., Noonan, F. P. & Merlino, G. (2003) *Oncogene* **22,** 3099–3112.
63. Smith, J. M. & Stump, K. C. (2000) *Contemp. Top. Lab. Anim. Sci.* **39,** 39–42.
64. Lefkaditou, E., Mytilineou, C. H., Maiorano, P. & D'Onghia, G. (2003) *J. Northw. Atl. Fish. Sci.* **31,** 431–440.
65. Avivi, A., Albrecht, U., Oster, H., Joel, A., Beiles, A. & Nevo, E. (2001) *Proc. Natl. Acad. Sci. USA* **98,** 13751–13756.
66. Avivi, A., Oster, H., Joel, A., Beiles, A., Albrecht, U. & Nevo, E. (2002) *Proc. Natl. Acad. Sci. USA* **99,** 11718–11723.
67. Avivi, A., Oster, H., Joel, A., Beiles, A., Albrecht, U. & Nevo, E. (2004) *J. Biol. Rhythm* **19,** 22–34.